Rong, Aiying; Lahdelma, Risto

An efficient model and algorithm for the transmission-constrained multi-site combined heat and power system

Published in:
European Journal of Operational Research

DOI:
10.1016/j.ejor.2016.09.002

Published: 01/01/2017

Document Version
Peer-reviewed accepted author manuscript, also known as Final accepted manuscript or Post-print

An efficient model and algorithm for the transmission-constrained multi-site combined heat and power system

Aiying Rong*, Risto Lahdelma

Department of Energy Technology
Aalto University
00076, Aalto, Finland

*Corresponding author: email: aiying.rong@aalto.fi
Tel: +358503415936, Fax: +358947023419

Abstract

This paper deals with the transmission-constrained multi-site combined heat and power (CHP) problem and formulates it as a linear programming (LP) model with a special structure. CHP systems are treated as an extension of power-only systems. Each site can be treated as a regional energy system to supply both heat and power. Heat demand is satisfied by local production while power demand can be satisfied by local generation plus power exchange over the power network. The challenge of this problem is that power transmission needs to be coordinated with both power and heat production in each site.

The transmission-constrained multi-site CHP system can be operated cost-efficiently according to hourly demand forecast for heat and power by coordinating production and transmission activities among different sites. An efficient network power Simplex algorithm is developed to this end. Numerical experiments with realistic test data show that the algorithm is 7 to 360 (with average 30) times faster than a commercial LP code.

Keywords: Linear programming; multi-site energy system; combined heat and power production; power transmission network; energy optimization.

1. Introduction

At present, fossil fuel depletion and mitigation of environmental impacts promote the improvement of energy efficiency in energy production and use. According to IEA (International Energy Agency) study on energy technology scenarios [1], improving energy efficiency contributes the largest share among all options for CO_2 emission reduction. Combined heat and power (CHP) production is a proven energy-efficient technology. In CHP, electric power and heat are produced simultaneously in a single integrated process, i.e., heat production and power production is interdependent in the CHP plant as shown in Figure 2 later in Section 2. The energy efficiency of the traditional condensing power plant is less than 40% while the overall efficiency of CHP production can be over 90% [2] because CHP can utilize otherwise wasted heat. For a fossil fuel based CHP plant, improved energy efficiency implies reduction of both fuel consumption and CO_2 emission. For a renewable biofuel based CHP plant, improved energy efficiency utilizes scarce biofuel more efficiently.

Currently, the deployment of CHP technology is not as extensive as it would be expected. CHP only accounts for around 10% of global power production [3]. However, in several European countries such as Denmark, Finland and the Netherlands, CHP technology has already contributed 30-50 % of national power production [3]. The European Union (EU) strongly encourages deployment of CHP technology [4] in conjunction with renewable energy sources (RES) such as wind, solar, geothermal and biomass. Both CHP and RES are foundations for the EU's energy policy for future low carbon energy systems [5]. Also, other countries, also outside EU, have adopted different support mechanisms to facilitate the deployment of CHP technologies [6]. It is expected that CHP systems will be prevalent all over the word in the future. By 2050, in the EU's high energy efficiency scenario, CHP is expected to account for 26 % of total EU electricity production and nearly two-thirds of energy input to CHP will be RES-based [7].

This paper studies the transmission-constrained multi-site CHP system shown in Figure 1. Power transmission refers to long distance transportation of electricity over high voltage (HV) lines (e.g. using the grid between cities or countries) [8]. Each site (Figure 1(a)) can contain any number of CHP production units, plus separate power and heat production units to meet given demand of power at power nodes and heat at heat nodes. Local distribution networks for power and heat are ignored in the modelling. Power-only systems can be treated as a special case of CHP systems, without heat

production and demand. On the other hand, the multi-site CHP systems can be viewed as an extension of the multi-site power-only systems, see e.g. [9] and [10].

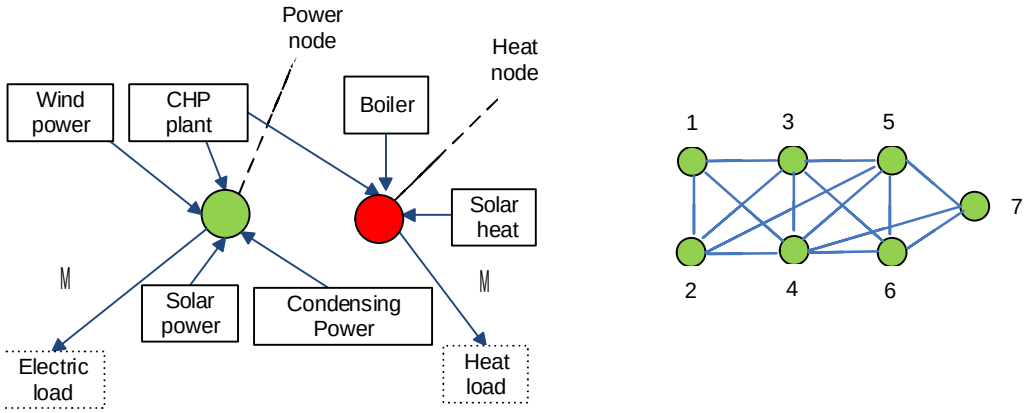

Figure 1. A transmission-constrained multi-site CHP system

Nowadays, interconnected regional energy systems [11] are common due to economic and financial benefits of interconnection [12]. Thus multi-site CHP systems can be interpreted in a broader context. A regional energy system can be any local energy system. Also EU aims at integrating national markets in the future to form the EU's energy union that can guarantee secure, competitive, reliable and low-carbon energy supply [13]. This means that interconnected systems will cover a wider region. This paper focuses on connection at a relatively high level, e.g. municipal or national level.

High penetration of intermittent RES into the power system has caused temporal and spatial imbalance between power supply and demand [14] for some countries and regions. One viable option to allow for higher utilization of RES is to coordinate power scheduling and power exchange among different regions [11]. When compared with power-only systems, CHP systems provide additional flexibility for achieving power grid balance. On one hand, the interdependence between heat and power production for CHP plants can be utilized to influence power production of CHP plants via adjusting heat production level [15] to accommodate more RES. On the other hand, electricity can be directly used to satisfy heat demand via electricity-heat transformation facilities such as heat pump to avoid or delay starting up heat demand driven CHP plants when there is large RES production [16]. In conjunction with heat storage, more RES can be utilized. This is equivalent to using heat storage to store electricity. It is known that heat storage is much cheaper than electric

storage [17]. Notice that globally heat accounts for 47 % of end use of energy [5]. Therefore, it is important to exploit the potential of CHP systems in balancing the power grid.

To the authors' knowledge, there is no research addressing transmission-constrained multi-site CHP systems. There are at least two reasons for this. Firstly, at present, penetration of CHP technology is not as wide as expected, as mentioned above, and thus CHP is often ignored when dealing with energy systems, especially with large-scale systems. Secondly, CHP systems are more complicated than power-only systems because CHP introduces a coupling between heat and power generation. This brings several challenges. On one hand, the coordination between heat and power generation is needed even for the small system (e.g. single-site CHP [18]). On the other hand, for the multi-site CHP system, power transmission is built upon the basis that heat demand in each site must be satisfied by local production. This means that the power transmission must be coordinated with both heat and power generation in each site. Also, it is difficult to dispatch CHP plants according to marginal power production costs that depend on heat generation level. Recently, [19] proposed a generic solution approach for the multi-site CHP system based on the decomposition framework, where the marginal power production costs of a single-site CHP system are computed according to parametric analysis [20]. Due to inherent inefficiency of parametric analysis, this approach is difficult to apply to a large system with a moderate planning horizon.

This paper pursues efficient solution of the hourly transmission- constrained multi-site CHP system in an integrated way. The hourly problem is the sub-problem of the unit commitment (UC) [21] that determines how the power transmission network is modelled. In the multi-site power scheduling context, the power transmission network is represented based on either DC (direct current) model [22] or network flow model [23, 24] as used in [10]. For dealing with the CHP system, usually energy flow and energy balance is focused without distinguishing between alternating current (AC) and DC or voltage level. Thus, the power transmission network in the current study is modeled based on the latter approach. Also, inherent coordination challenges for power transmission and power and heat coupling in CHP plants justify this choice. Numerical experiments [21] showed that it is even difficult to solve some daily scheduling instances of UC for the network flow model based transmission-constrained 5-site CHP problem using the standard solver with 0.5% relative gap. The efficient solution of the hourly model is important for at least two reasons. Firstly, for solving more advanced problems incorporating UC [25, 26] or/and storage [27] for CHP systems in the multi-site power scheduling context, different variants of hourly models need to be solved iteratively many times for a given horizon (e.g. daily). Secondly, for dealing with uncertainties caused by intermittent

RES based on stochastic optimization, multiple scenarios need to be evaluated for a given horizon. In each scenario [28], a variant of scheduling problem mentioned in the first case needs to be solved.

The contributions of this paper are summarized as follows. Firstly, it is the first attempt to deal with the transmission-constrained multi-site CHP system that can cover a broad category of interconnected energy systems. Secondly, the hourly model is formulated as a linear programming (LP) model with a special structure. Thirdly, a specialized efficient two-stage network power Simplex (NPS) algorithm is developed by jointly exploiting the special structure of CHP production model [18, 29] and the network flow model [23, 24]. The first stage can provide an advanced solution by solving an easy problem without power network. Finally, the efficiency of the algorithm is evaluated according to realistic data and plant models of Finnish energy companies.

The paper is organized as follows. Section 2 formulates the hourly transmission-constrained multi-site CHP system optimization model. Section 3 reviews the generic Revised Simplex algorithm with upper bounds for solving LP problems. Section 4 presents the NPS algorithm. Section 5 presents numerical experiments with realistic test models. The four appendices collect the procedure for generic revised Simplex algorithm, sub-procedures for implementing NPS as well as a detailed pivot process.

2. Problem formulation

The objective of the transmission-constrained multi-site CHP system optimization is to minimize total heat and power production costs as well as power transmission costs while satisfying the heat and power demand. The heat demand is met by local production while the power demand is met by local generation and possible power transmission via a power network.

As shown in Figure 1(a), CHP production is a hybrid system, which may contain both thermal processes such as condensing power plants and heat-only boilers as well as RES based technology such as wind power, solar power and solar heat. Thermal processes can be based on fossil fuels, nuclear energy and renewable biomass. CHP plants follow thermal processes. Considering the geographical dispersion for different sites and high level (municipal, national) interconnections, in practice, only the sites close to each other have a direct power transmission line connection and the entire system is an interconnected system. The power network is modelled according to network flow model [23, 24], similar to [10]. In the model, only power nodes in Figure 1 (a) are explicitly considered and heat nodes are simply represented as the heat balance of the physical site. Two nodes (regional power systems) are adjacent if they are connected by an *arc* (transmission line). These two

nodes are called incident nodes of the arc [24]. Let $d(j)$ denote the degree of node j, which is the number of arcs incident on node j. The power transmission network in the current study is bidirectional, i.e., if there is an arc from i to j, there is also an arc from j to i.

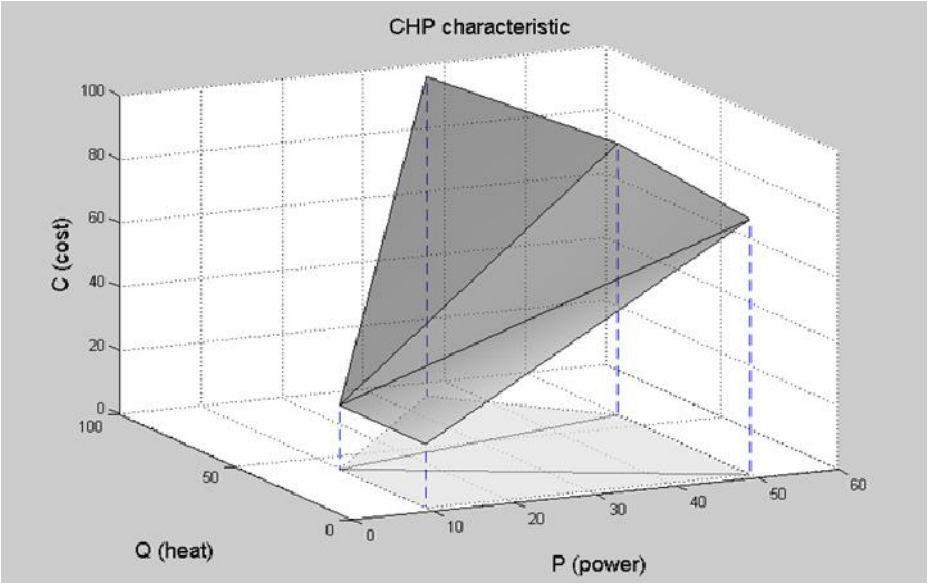

Figure 2 feasible region of a CHP plant (P= power; Q= heat; C= production cost) from [30]

For CHP modeling, we assume that plant characteristic is convex as in [29]. Figure 2 [30] shows the feasible characteristic operating region of a convex plant. The corner points are called the extreme points of the region. The convex characteristic can be represented as the *convex combination* of extreme points [20]. It is worth mentioning that the convexity assumption is not as limiting as it seems as described in [29]. In [31], it is mentioned that convexity assumption is sometimes justified even when the plant characteristic is non-convex [32, 33]. In addition, power-only and heat-only plants are treated as special cases of CHP plants with zero q- or p-component, respectively. It is also possible that a CHP plant has some extreme points with zero q- and/or p-component. Our notation is defined as follows:

Indices

i,j site index,

(i,j) power arc,

p, q superscripts/subscripts or prefixes for power and heat in the system,

u plant index.

Index sets

F set of generation and demand sites (nodes),

A set of arcs A { $(i,j) : i,j \in F, i \neq j$ },

J set of extreme points of the operating regions of all plants ($J = \bigcup_{i \in F} J_i$),

J_i set of extreme points of the operating regions of plants at site i,

J_u set of extreme points of the operating region of plant u,

U set of all plants. ($J = \bigcup_{i \in F} U_i$),

U_i set of plants at site $i \in F$,

Parameters

(c_j, p_j, q_j) extreme point $j \in J_u$ of the operating region of plant u (cost, power, heat),

$c_{i,j}$ transmission cost on arc (i,j),

$c_{i,p\pm}$ power surplus/slack cost at site i,

$c_{i,q\pm}$ heat surplus/slack cost at site i,

$g_{i,j}$ capacity of arc (i,j),

P_i power demand at site i,

Q_i heat demand at site i.

Decision variables

x_j decision variables used for encoding the operating level of each plant in terms of extreme points of the operating region,

$x_{i,q\pm}$ heat surplus/slack quantity at site i,

$x_{i,p\pm}$ power surplus/slack quantity at site i,

$y_{i,j}$ power flow on arc (i,j).

The hourly model is formulated as

$$\text{Min} \sum_{j \in J} c_j x_j + \sum_{i \in F} (c_{i,q+} x_{i,q+} + c_{i,q-} x_{i,q-} + c_{i,p+} x_{i,p+} + c_{i,p-} x_{i,p-}) + \sum_{(i,j) \in A} c_{i,j} y_{i,j} \qquad (1)$$

s.t.

$$\sum_{j \in J_u} x_j = 1, \qquad u \in U, \qquad (2)$$

$$\sum_{j \in J_i} q_j x_j - x_{i,q+} + x_{i,q-} = Q_i, \qquad i \in F, \qquad (3)$$

$$\sum_{j \in J_i} p_j x_j + \sum_{\{j|(j,i) \in A\}} y_{j,i} - \sum_{\{j|(i,j) \in A\}} y_{i,j} - x_{i,p+} + x_{i,p-} = P_i, i \in F, \quad (4)$$

$$x_j \geq 0, \quad j \in J, \quad (5)$$

$$x_{i,q\pm}, x_{i,p\pm} \geq 0, \quad i \in F, \quad (6)$$

$$0 \leq y_{i,j} \leq g_{i,j}, \quad (i,j) \in A, \quad (7)$$

In the above formulation, objective (1) is to minimize the total production and transmission cost as well as possible power and heat surplus/slack penalty. Constraints (2) together with (5) represent the convex combination of extreme points of the operating region of each plant. Constraints (3) state that the heat demand in each site is met by local production. Constraints (4) state that the power demand in each site is met by local generation and power exchange via power network. In both (3) and (4) the surplus and slack variables for heat and power are introduced to guarantee that feasible solutions exist for any levels of demand. Constraints (7) enforce transmission capacity constraints for each arc. The major purpose of the power surplus/slack variables is to determine which site does not have sufficient power generation capacity and which site has surplus power when the power transmission network is absent. The power surplus/slack variables should be out of the basis when power transmission network is present. From (3) and (4), it can be seen that there are $|F|$ heat balances and power balances, respectively. To distinguish between heat and power balances, for site *j*, the rows corresponding to heat and power balances are called *j*(*q*)-rows and *j*(*p*)-rows, respectively. Accordingly, constraints (2) corresponding to plants are called *u*-rows.

3. Generic revised simplex with upper bounds

A variant of Revised Simplex algorithm without upper bounds was applied in [29], while [18] used a variant with upper bounds. Here arc capacities (7) need to be considered explicitly and thus the variant with upper bounds is needed. The major purpose for this review is to introduce notation which facilitates the presentation of NPS algorithm later. The canonical form of the LP problem is

$$\min z = cx$$

s.t.

$$\mathbf{A}x = b, \quad (8)$$

$$0 \leq x \leq x^{max},$$

where *z* is the linear objective function to be minimized in terms of the variable vector *x* and *c* is the row vector of cost coefficients, **A** is the *m´ n* constraint matrix (*m* and *n* refer to the number of

constrains and number of variables, respectively). b is the right-hand-side vector, and x^{max} is the upper bound vector for decision variables. In this formulation, possible slack and surplus variables are included in x.

For solving the problem using Simplex, **A**, x and c are partitioned as

$$\mathbf{A} = [\mathbf{B} \mid \mathbf{N}],\ x = \begin{bmatrix} x^B \\ x^N \end{bmatrix},\ c = [c^B \mid c^N], \tag{9}$$

where **B** is the non-singular basis matrix, **N** is the non-basic matrix, x^B is the vector of basic variables, x^N is the vector of non-basic variables, and c^B and c^N are the cost coefficients for the basic and non-basic variables. In a basic solution, the non-basic variables are set at either their lower bounds (zero) or at their upper bounds (x^{max}), then the values for the basic variables are determined so that the constraints are satisfied, i.e.,

$$x^B = \mathbf{B}^{-1}(b - \mathbf{N}x^N) = \mathbf{B}^{-1}\beta, \tag{10}$$

$$\beta = b - Nx^N. \tag{11}$$

The basic solution is *feasible* when the basic variables are within their bounds $0 \le x^B \le x^{B,max}$ (any non-basic variable is by definition feasible as it is on its either bound). Introducing row vector ρ, called dual values of the constraints, such that

$$\rho = c^B\mathbf{B}^{-1}, \tag{12}$$

and substituting x^B and ρ into the objective function yields

$$z = c^Bx^B + c^Nx^N = \rho b + dx^N, \tag{13}$$

where ρb is a constant and

$$d = c^N - \rho\mathbf{N} \tag{14}$$

is the row vector of the *reduced costs* for non-basic variables. The reduced costs indicate how z changes when non-basic variables are moved away from their bounds while maintaining all the constraints valid. The solution is optimal if the *optimality condition* holds

$d_j \ge 0$ for all non-basic variables that are at their lower bound and

$d_j \le 0$ for all non-basic variables that are at their upper bound.

Any non-basic variable that does not satisfy the optimality condition will improve the objective function value when entering the basis. If the value of a non-basic variable x_j^N is changed by Δx_j^N, then, according to (10), the basic variable vector changes by $-y\Delta x_j^N$, where we have introduced the *pivot column*

$$y = \mathbf{B}^{-1}\,\mathbf{N}_{\cdot j}, \tag{15}$$

and $\mathbf{N}_{\cdot j}$ is the column vector corresponding to x_j^N in **A.**

The maximum allowed change Δx_j^N for the entering variable must be chosen such that the feasibility of all basic variables is maintained, i.e.,

$$0 \le x^B - y\Delta x_j^N \le x^{B,\max}. \tag{16}$$

and one of the basic variables reaches its either bound, i.e., leaves the basis.

The generic Revised Simplex algorithm is presented in Appendix A.

4. Network Power Simplex

The network power Simplex (NPS) follows the paradigm of the generic revised Simplex algorithm with upper bounds. The algorithm identifies the special structure of the basis by combining the special structure of the multi-site CHP production model [29] with the special structure of network flow model [23, 24] in order to compute the vectors x^B, p, and y efficiently. In principle, x^B, p, and y are solved from the equation systems:

$$\mathbf{B}x^B = \beta \tag{17}$$

$$p\mathbf{B} = c^B, \tag{18}$$

$$\mathbf{B}y = \mathbf{N}_{\cdot j}. \tag{19}$$

For the current problem, two important issues need to be handled. The first one is to decompose **B** into smaller blocks so that the equation systems can be solved efficiently, as was done in [18] and [29] for problems with different structures. The second one is to handle the coupling of flow variables between two sites in the computational process so that the coupling issue can also be

addressed efficiently. The major motivation for exploiting the structure of the basis is to speed up the solution process by avoiding manipulation of the inverse of the large matrix. In the following, we describe the structure of the model and the basis.

4.1 Structure of the model

Figure 3 illustrates the structure of the model. Subscripts 1, ...,$|F|$ refer to demand sites, where each site has both heat and power balances. The structure of the u-row and the $j(q)$-row is the same as that in [29] because constraints (2) and (3) remain the same. The structure of the $j(p)$-row introduces coupling between two sites by flow variables (constraints (4)). **A**-matrix remains sparse, as that in [29], because each column for the flow variables contains only two non-zero coefficients. The number of rows in the **A**-matrix of the LP problem is $m = |U|+2|F|$ and the number of columns is $n = |J|+2|F|+n_f$, where $n_f = \sum_{j \in F} d(j)$ is total number of flow variables. Both power network ($j(p)$-rows) and CHP production constraints (u-rows) have a special structure. This means that it is possible to implement Simplex algorithm more efficiently if coupling between production and transmission systems is handled properly.

4.2 Structure of the basis

As shown in Figure 4, the overall structure of basis **B** is almost the same as that in [29]. The major changes are reflected in two aspects because of the introduction of flow variables. Firstly, the structure and size of **D** ($v' \times v$) changes significantly as shown later in (29)-(31), where $|F|+1 \le v \le 4|F|$. Secondly, the dimensions of $\mathbf{p}^B$, $\mathbf{q}^B$ and matrix $\mathbf{0}$ between $\mathbf{q}^B$ and $\mathbf{p}^B$ will be changed. The **B** is formed by rearranging the rows and columns of **B** to facilitate exploiting the structure for solving the equation systems (17)-(19) efficiently.

For u-rows and $j(q)$-rows, the choices of basic variables are the same as those in [29], while the choices of $j(p)$-row basic variables are different. The u-row basic variables are from plant u. The $j(q)$-row basic variables can be either from the plant at site j or heat surplus/slack variables $x_{j,q\pm}$. For the $j(p)$-row basic variables, there are three possibilities: from the plant at site j, from power surplus/slack variables $x_{j,p\pm}$ and from flow variables incident at site j. Consequently, each plant u can contribute one to three basic variables.

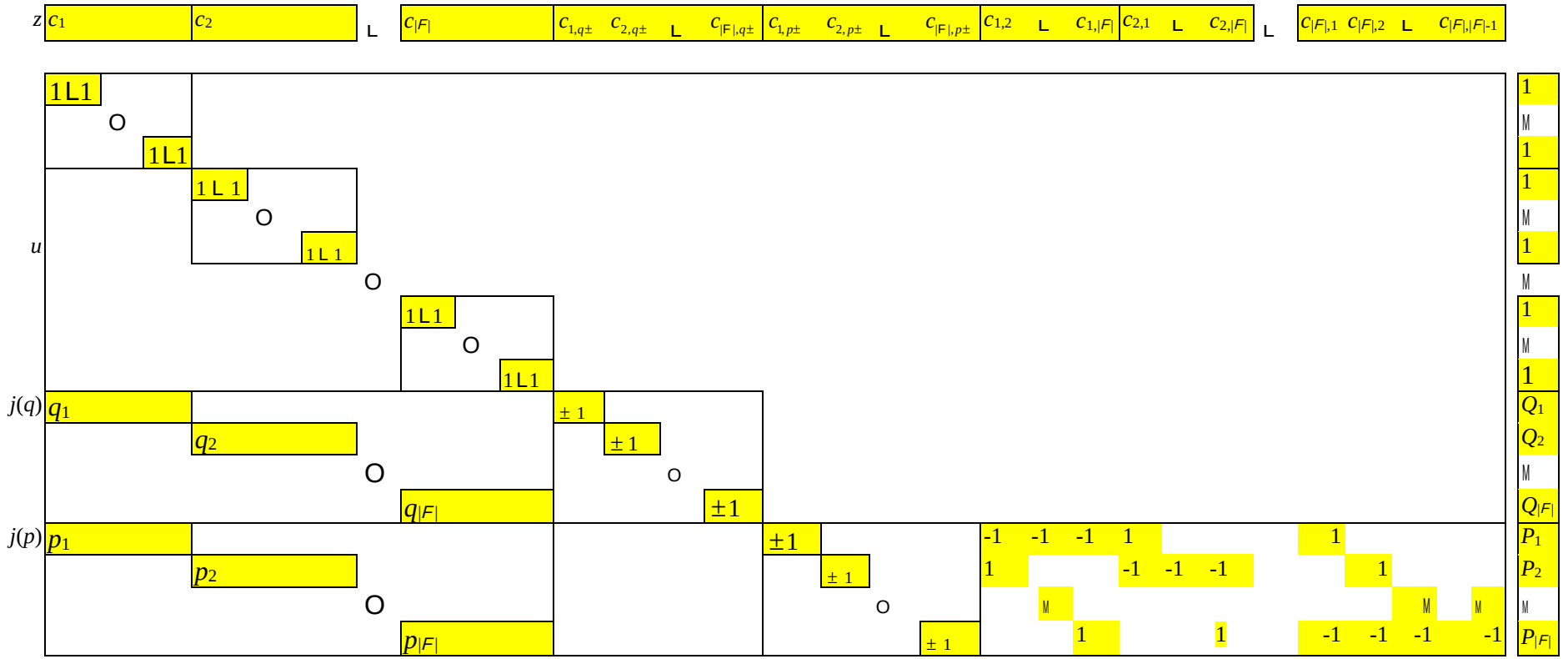

Figure 3. Structure of integrated multi-site CHP production and power transmission problem

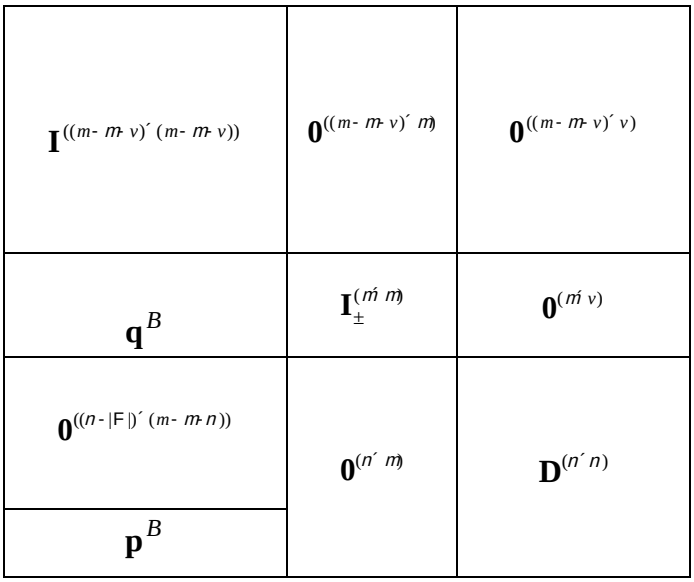

Figure 4. The structure of the basis

The left upper corner $\mathbf{I}^{((m-m+v)\times(m-m+v))}$ diagonal matrix corresponds to the structure of partial *u*-row basic variables when plant *u* contributes only one basic variable. The middle $\mathbf{I}_{\pm}^{(m\times m)}$ diagonal matrix corresponds to the case when *q*(*j*)-row basic variables are from heat surplus /slack variable $x_{j,q\pm}$ and *j*(*p*)-row basic variables are from the flow variable. The right bottom $\mathbf{D}^{(n\times n)}$ matrix corresponds to two cases according to the choices of *q*(*j*)- row basic variables. The first case: the *q*(*j*)-row basic variables are from heat surplus /slack variable $x_{j,q\pm}$, and the *j*(*p*)-row basic variables are not flow variables. The second case: the *q*(*j*)-row basic variables are from plants, and *j*(*p*)-row basic variables can have three possibilities as just discussed. According to Figure 4, **B** can be written as below.

$$\mathbf{B}=\begin{bmatrix}\mathbf{I} & & \\ \mathbf{E}_1 & \mathbf{I}_{\pm} & \\ \mathbf{E}_2 & \mathbf{0} & \mathbf{D}\end{bmatrix}, \tag{20}$$

The formulae for computing ρ and *y* are the same as those in [29]. These formulae are still needed to present the NPS algorithm later. To compute ρ, ρ and c^B are partitioned into three parts and equation (18) can be written as

$$[p_1 \quad p_2 \quad p_3]\begin{bmatrix} \mathbf{I} & & \\ \mathbf{E}_1 & \mathbf{I}_{\pm} & \\ \mathbf{E}_2 & \mathbf{0} & \mathbf{D} \end{bmatrix} = [c_1^B \quad c_2^B \quad c_3^B]. \tag{21}$$

The p_3, p_2, and p_1 are obtained in sequence from

$$p_3\mathbf{D} = c_3^B, \tag{22}$$

$$p_2 = \pm c_2^B, \tag{23}$$

$$p_1 = c_1^B - p_2\mathbf{E}_1 - p_3\mathbf{E}_2. \tag{24}$$

Computing p_3 requires solving an equation system involving **D**. p_2 can be computed independently and trivially. After that, p_1 can be obtained trivially.

Similarly, to compute y, y and $\mathbf{N}_{\cdot j}$ are partitioned into three parts and equation (19) can be written as

$$\begin{bmatrix} \mathbf{I} & & \\ \mathbf{E}_1 & \mathbf{I}_{\pm} & \\ \mathbf{E}_2 & \mathbf{0} & \mathbf{D} \end{bmatrix}\begin{bmatrix} y_1 \\ y_2 \\ y_3 \end{bmatrix} = \begin{bmatrix} N_{\cdot j1} \\ N_{\cdot j2} \\ N_{\cdot j3} \end{bmatrix}. \tag{25}$$

Then y_1, y_2 and y_3 are obtained in sequence

$$y_1 = N_{\bullet j1}, \tag{26}$$

$$y_2 = \pm(N_{\bullet j2} - \mathbf{E}_1 y_1), \tag{27}$$

$$\mathbf{D}y_3 = N_{\bullet j3} - \mathbf{E}_2 y_1. \tag{28}$$

The two first parts of y can be computed trivially. Computing y_3 requires solving an equation system involving **D**. The x^B is solved from (17) similarly as y but with β as the right hand side instead of $\mathbf{N}_{\cdot j}$. For incremental basis update (Section D. 3.1 in Appendix D), there is a slight difference between calculating x^B and y as shown in Section D.3.2.

It is clear that the essence of NPS deals with the issue of how to solve the $v \times v$ equation systems (22) and (28) involving **D**. Next, the structure of **D** is explored and then the algorithm for solving (22) and (28) is presented.

4.3 Structure of **D**

The size of **D** is not the sole factor to affect the complexity of solving equation systems involving **D**. If no flow variables are in the basis, the size of **D** can be $4|F|\times 4|F|$ because the maximal size of matrix block related to **D** for the individual site is 4×4, as discussed in [18] and illustrated in (29) (the second block). However, this case corresponds to the easiest situation when there is no coupling between sites. Each individual site can be solved by PS [18]. As the number of basic flow variables increases, the **D** evolves into structure (30), where certain sites are coupled by basic flow variables at the $j(p)$-row. In the matrix, the elements in yellow correspond to the pivot elements for the corresponding rows. The possible smallest size for **D** is $(|F|+1) \times (|F|+1)$, which corresponds to the case where there are $(|F|-1)$ basic flow variables and one non-flow basic variable at the $j(p)$-row is surplus/slack variable and all basic variables at the $j(q)$-row are surplus/slack variables. This is equivalent to the pure network case [23, 24], which is also a relatively easy case to solve. Coupling between production and transmission is the major issue for handling **D** efficiently. In the following, the pattern of basic flow variables is discussed. In (29) and (30), $j(.)$ denotes rearranged sites.

It is known that the structure of the feasible flow variables for the pure network problem is a *tree* [23, 24], which includes all of nodes for the problem. A tree is a connected graph with no cycles. For linear network optimization problem involving flow variables, the pattern of feasible basic flow variables should have a tree-like non-cyclic structure because basic variables must be independent of each other to guarantee non-singularity of the basis.

For the current problem the pattern of feasible basic flow variables should be a forest [34], as shown in Figure 5(a). The forest consists of multiple disjoint trees. In Figure 5(a), there are three trees, and the nodes marked in grey are the root nodes. A root node has at least two functions. Firstly, it is the starting node for constructing a tree (Algorithm C.2 in Appendix C). Secondly, in the optimization problem, it is a reference node for calculating the dual values of the remaining nodes (π in (18)) because each node has a unique *path* to the root node. A path is a sequence of nodes connected by arcs [24].

There are two differences between the pure network optimization in [23, 24] and the power network in the current study. Firstly, all variables in the pure network optimization are flow variables while the variables in the current problem contain both production variables and flow variables because all nodes

D =

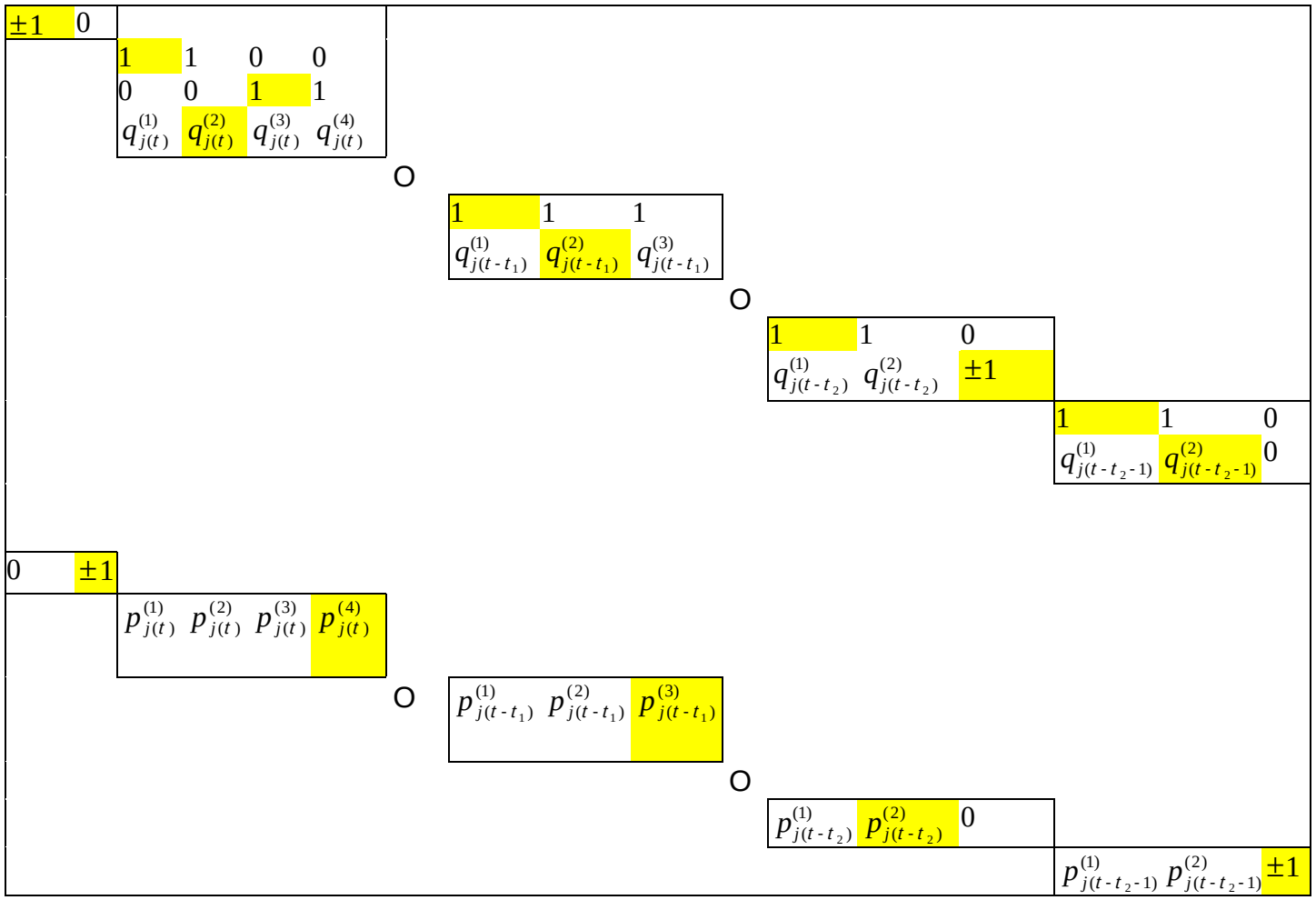
±1 0
1 1 0 0
0 0 1 1
$q^{(1)}_{j(t)}$ $q^{(2)}_{j(t)}$ $q^{(3)}_{j(t)}$ $q^{(4)}_{j(t)}$
O
1 1 1
$q^{(1)}_{j(t-t_1)}$ $q^{(2)}_{j(t-t_1)}$ $q^{(3)}_{j(t-t_1)}$
O
1 1 0
$q^{(1)}_{j(t-t_2)}$ $q^{(2)}_{j(t-t_2)}$ ±1
1 1 0
$q^{(1)}_{j(t-t_2-1)}$ $q^{(2)}_{j(t-t_2-1)}$ 0
0 ±1
$p^{(1)}_{j(t)}$ $p^{(2)}_{j(t)}$ $p^{(3)}_{j(t)}$ $p^{(4)}_{j(t)}$
O
$p^{(1)}_{j(t-t_1)}$ $p^{(2)}_{j(t-t_1)}$ $p^{(3)}_{j(t-t_1)}$
O
$p^{(1)}_{j(t-t_2)}$ $p^{(2)}_{j(t-t_2)}$ 0
$p^{(1)}_{j(t-t_2-1)}$ $p^{(2)}_{j(t-t_2-1)}$ ±1

(29)

D=

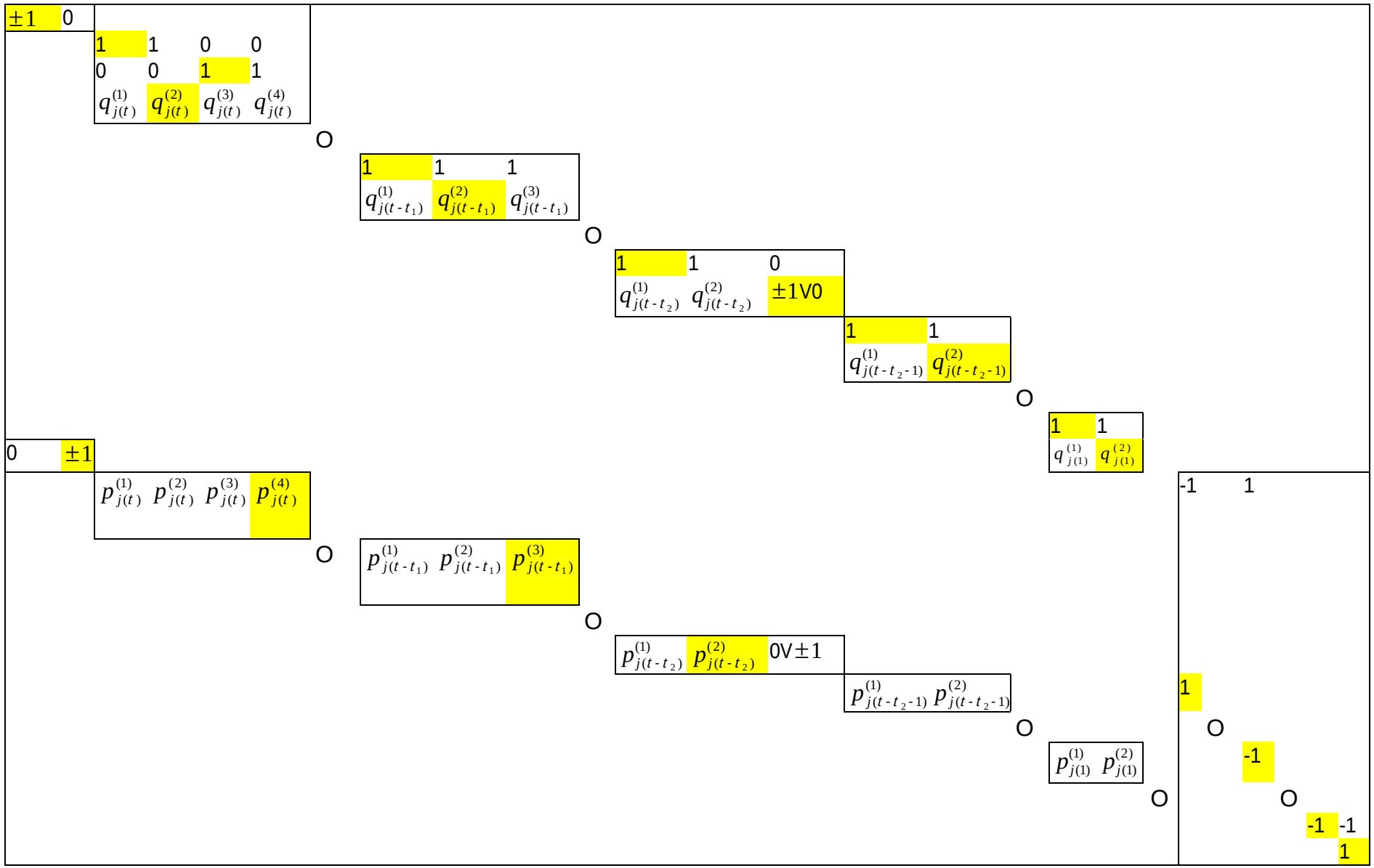
±1 0
1 1 0 0
0 0 1 1
$q^{(1)}_{j(t)}$ $q^{(2)}_{j(t)}$ $q^{(3)}_{j(t)}$ $q^{(4)}_{j(t)}$
O
1 1 1
$q^{(1)}_{j(t-t_1)}$ $q^{(2)}_{j(t-t_1)}$ $q^{(3)}_{j(t-t_1)}$
O
1 1 0
$q^{(1)}_{j(t-t_2)}$ $q^{(2)}_{j(t-t_2)}$ ±1V0
O
1 1
$q^{(1)}_{j(t-t_2-1)}$ $q^{(2)}_{j(t-t_2-1)}$
O
1 1
$q^{(1)}_{j(1)}$ $q^{(2)}_{j(1)}$
O
0 ±1
$p^{(1)}_{j(t)}$ $p^{(2)}_{j(t)}$ $p^{(3)}_{j(t)}$ $p^{(4)}_{j(t)}$
O
$p^{(1)}_{j(t-t_1)}$ $p^{(2)}_{j(t-t_1)}$ $p^{(3)}_{j(t-t_1)}$
O
$p^{(1)}_{j(t-t_2)}$ $p^{(2)}_{j(t-t_2)}$ 0V±1
O
$p^{(1)}_{j(t-t_2-1)}$ $p^{(2)}_{j(t-t_2-1)}$
O
$p^{(1)}_{j(1)}$ $p^{(2)}_{j(1)}$
O
-1 1
1
O
-1
O
-1 -1
1

(30)

have generation capability. Secondly, the pure network optimization with w nodes (thus w constraints) has only (w-1) independent constraints because one constraint can be represented as the linear combination of remaining constraints according to the requirements of flow balance. Consequently, there are only (w-1) basic (flow) variables. For the current problem, w nodes correspond to w independent power balances and thus must have w basic variables.

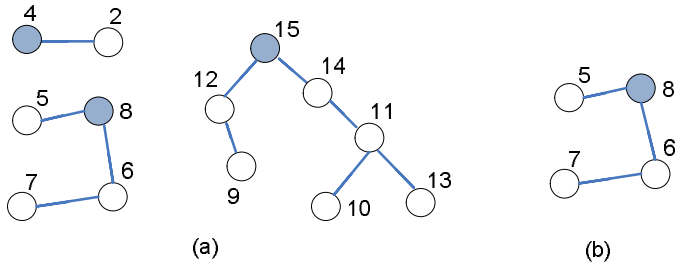

Figure 5. Pattern of feasible basic flow variables for a 15-site problem

Lemma 1. The pattern for basic feasible flow variables for the current problem assumes a tree or a forest structure as shown in Figure 5 (a). Each tree contains exactly one node whose basic variable at the $j(p)$-row is not a flow variable.

Proof: Assume that a tree consists of w nodes and the number of arcs (flow variables) in the tree should be w-1. There are w $j(p)$-rows corresponding to w nodes. Thus, the basis must contain w basic variables. This means that one basic variable must be non-flow variables. •

It can be seen from Lemma 1 that there exists exactly one node whose basic variable is not a flow variable in a tree. This node is an ideal candidate for the root node for several reasons though other nodes can also act as a root node. Firstly, it is easy to identify this node and know beforehand how many trees are contained in the basis (refer to Algorithm B.1 in Appendix B). Secondly, p values of this node can be computed independently (see Algorithm C.1 in Appendix C). Finally, this node can guarantee the connection of nodes within the tree and separation between trees. Consequently, the **D** decomposes into multiple independent sites and multiple disjoint site clusters. Each site cluster is associated with a tree.

$$\mathbf{D} = \left\lfloor \mathbf{D}_1 \quad \llcorner \quad \mathbf{D}_q \quad \mathbf{\Gamma}_1 \quad \llcorner \quad \mathbf{\Gamma}_r \right\rfloor, \tag{31}$$

where θ is the number of independent sites and r the number of non-degenerate trees with $|\mathcal{G}_i| \geq 2$ (i=1,…, r) in **D**, $\theta + r = |F| - \sum_i (|\mathcal{G}_i| - 1)$, $0 \leq \theta \leq |F|$. For the example shown in Figure 5 (a), let $|F|$= 15, then θ =2 and r =3. $|\mathcal{G}_1|$ =2, $|\mathcal{G}_2|$ =4, and $|\mathcal{G}_3|$ = 7. There are two independent sites: 1 and 3. For the independent sites, p_3 and y_3 can be obtained efficiently by using the procedure in PS [18]. The major issue in computing p_3 and y_3 is how to handle the tree efficiently.

Based on the basis structure (20), **D** is the only block that introduces possible coupling in the basis. If **D** is decomposable, then the basis can decompose following the structure of **D**. Therefore, **B** can be represented as

$$\mathbf{B} = \begin{bmatrix} \mathbf{B}_1 & \cdots & \mathbf{B}_q & \mathcal{L}_1 & \cdots & \mathcal{L}_r \end{bmatrix}, \tag{32}$$

where $\mathcal{L}_i$ (i= 1,…, r) is a component of **B** associated with tree $\mathcal{G}_i$.

$$\mathcal{G}_s = \begin{array}{|c|ccc|ccc|ccc|ccc|} \hline & 1 & 1 & 1 & & & & & & & & & \\ & q^{(1)}_{j_s(1)} & q^{(2)}_{j_s(1)} & q^{(3)}_{j_s(1)} & & & & & & & & & \\ \hline & & & & 1 & 1 & & & & & & & \\ & & & & q^{(1)}_{j_s(2)} & q^{(2)}_{j_s(2)} & & & & & & & \\ \hline & & & & & & 1 & 1 & & & & & \\ & & & & & & q^{(1)}_{j_s(3)} & q^{(2)}_{j_s(3)} & & & & & \\ \hline & p^{(1)}_{j_s(1)} & p^{(2)}_{j_s(1)} & p^{(3)}_{j_s(1)} & & & & & & & -1 & 1 & \\ \hline & & & & p^{(1)}_{j_s(2)} & p^{(2)}_{j_s(2)} & & & & & 1 & & 1 \\ & & & & & & p^{(1)}_{j_s(3)} & p^{(2)}_{j_s(3)} & & & & -1 & \\ \hline & & & & & & & & & & & & -1 \\ \hline \end{array} \tag{33}$$

The tree can be dynamically identified by first identifying the root of the tree (see Algorithm B.1 in Appendix B). The root is determined by checking the incident nodes for the basic flow variable. If the basic variable for one incident node is not a flow variable, then this node is the root node. For a given root, a variant of the depth-first search (DFS) algorithm [23] (Algorithm B.2 in Appendix B) is used to identify the remaining nodes in the tree. DFS traverses the tree, starting at the root and exploring the tree as far as possible before backtracking. On the path from the root to node j, node i visited immediately

before node j is called the predecessor of node j. The connection of the nodes in the tree is uniquely determined if the predecessors of the nodes are known.

To exhibit a given tree (G_s) structure, the indices of rows and columns of **B** are rearranged. Without loss of generality, let w_s denote the number of nodes (sites) in a tree and $j_s(i)$ (i =1,…, w_s) the nodes in the tree, where $j_s(1)$ is the root. Let $\mathbf{R}_s$ denote $a \times a$ (a = 2, 3, 4) matrix of $j_s(1)$ ((29) shows five cases for $\mathbf{R}_s$.) Matrix (33) shows one possible tree structure for the tree in Figure 5(b). The size of matrix $m_{G_s} = a+2 \times 2+(w_s-1)=10$. Let $g_s(i)$ be the predecessor of $j_s(i)$ on the path from the root to $j_s(i)$, and $d_s(i)$ the degree of $j_s(i)$. For Figure 5(b), $w_s = 4$, j_s =[8,5,6,7], g_s =[-1,8,8,6] and d_s =[2,1,2,1].

Therefore, for solving (22) and (28) efficiently, it is essential to efficiently solve equations associated with the tree.

4.4 Solving equations systems associated with G_s

Solving the equations system associated with a tree is crucial for solving equation systems (17) – (19). The solution efficiency of the tree determines the solution efficiency of the NPS algorithm. The detailed algorithm procedures are presented in Appendix C. The main idea of the algorithm is to determine the sequence of solving small matrix blocks so that p_3 and y_3 associated with the tree can be determined in sequence based on values of p_3 and y_3 that have been determined. According to Algorithm C.1 in Appendix C, the sequence for obtaining p_3 is to solve a rows of the root node first, then the $j_s(p)$-row associated with flow variables at sites $j_s(i)$ (i=2,…, w_s) and finally the corresponding $j_s(q)$-row and u_s-row of sites $j_s(i)$ (i=2,…, w_s). The above sequence justifies the selection of the root node as discussed in Section 4.3 because the dual values associated with the node can be obtained independently. According to Algorithm C.2 in Appendix C, the sequence of obtaining y_3 takes the inverse order of obtaining p_3.

The algorithms mainly rely on proper indexing to implement special structure. Taking the tree in (33) as an example, if p_3=[$p_{3,1}$, $p_{3,2}$, $p_{3,3}$, $p_{3,4}$, $p_{3,5}$, $p_{3,6}$, $\boldsymbol{p_{3,7}}$, $p_{3,8}$, $p_{3,9}$, $p_{3,10}$], then c_3=[$c_{3,1}$, $c_{3,2}$, $\boldsymbol{c_{3,7}}$, $c_{3,3}$, $c_{3,4}$, $c_{3,5}$, $c_{3,6}$, $c_{3,8}$, $c_{3,9}$, $c_{3,10}$], y_3=[$y_{3,1}$, $y_{3,2}$, $\boldsymbol{y_{3,7}}$, $y_{3,3}$, $y_{3,4}$, $y_{3,5}$, $y_{3,6}$, $y_{3,8}$, $y_{3,9}$, $y_{3,10}$]^T and l_3= [$l_{3,1}$, $l_{3,2}$, $l_{3,3}$, $l_{3,4}$, $l_{3,5}$, $l_{3,6}$, $\boldsymbol{l_{3,7}}$, $l_{3,8}$, $l_{3,9}$, $l_{3,10}$]^T. It is worth paying attention to the positions of $\boldsymbol{c_{3,7}}$ and $\boldsymbol{y_{3,7}}$ in vectors c_3 and y_3, respectively.

4.5 Pivot for forming a non-singular basis and incremental basis update

Any entering variable from one site can cause the row from the different site to leave because flow variables couple between different sites. The pivot is more complicated than single-site CHP production optimization [18] and multi-site CHP production optimization [29]. The detailed pivot process is described in Section D.2 in Appendix D. Two ways of basis update can be considered. One is called full (normal) basis update where the basis is updated considering all sites. The other is called incremental basis update where the basis is updated only considering the sites affected by the pivot. For detailed information, refer to Section D.3 in Appendix D.

4.6 Network Power Simplex (NPS) algorithm

Two NPS algorithms are developed. The first one is the direct adaption of Algorithm A (a generic Simplex algorithm in Appendix A), called DNPS. The second one, called TNPS, applies a two-stage approach. In the first stage, the problem without power network is considered. Each individual site is solved by PS [18] to obtain an advanced solution. If all sites have surplus electric power or lack of power, the solution is optimal to the original problem. Otherwise, the second stage is used to solve the original problem with power network using the same Simplex procedure as DNPS applies. In this case, the solution for the first-stage problem can be treated as the initial solution for NPS algorithm.

Algorithm 1 *DNPS algorithm*

Step 1. Initialization: start from some feasible solution (9) by considering only plant variables and surplus/slack variables.

Step 2. Identify decomposable structure of the basis $\mathbf{B}=\lfloor \mathbf{B}_1 \ \llcorner \ \mathbf{B}_q \ \ \mathbf{\Sigma}_1 \ \llcorner \ \mathbf{\Sigma}_r \rfloor$ according to basic variables at the $j(p)$-row based on algorithms B.1 and B.2 in Appendix B.

Step 3. Calculate x^B (10) from (17) according to PS [18] for site 1 to θ, and procedures described in (26) to (28) and Algorithm C.2 in Appendix C for tree 1 to r; Calculate p from (18) according to PS [18] for site 1 to θ, and procedures described in (22) to (24) and Algorithm C.1 in Appendix C for tree 1 to r; Calculate d (14).

Step 4. Find a variable x_j^N to enter the basis such that z improves. The condition is $d_j<0$ (>0) for variables at lower (upper) bound. If there is no such variable, stop with optimal x^B.

Step 5. Compute the pivot column y from (19) according to PS [18] for site from 1 to θ, and procedures described in (26) to (28) and Algorithm C.2 in Appendix C for tree 1 to r.

Step 6. Find the variable to leave the basis such that feasibility is maintained. The leaving variable is the one that according to (16) reaches its upper or lower bound first when the entering variable is moved away from its bound. If there is no such variable, stop with an unbounded solution.

Step 7. Update the basis and go to **Step 2.**

Algorithm 2 TNPS algorithm

Step 1. Solve site 1 to $|F|$ without transmission network using PS [18], if all sites have power surplus or lack power, stop with the optimal solution; otherwise, continue to **Step 2**.

Step 2. Repeat Steps 2 to 7 of Algorithm 1.

Both the DNPS and TNPS algorithms can adopt the incremental basis update scheme described in Section D. 3.1 in Appendix D. The way to solve the equation systems (17)-(19) is described in D.3.2 in Appendix D.

5. Computational experiments

To evaluate the effectiveness of the two- stage network Power Simplex (TNPS) algorithm, two versions of the algorithms were implemented. The first version (TNPS1) and the second version (TNPS2) adopted the full and incremental basis update schemes, respectively as described in Section D.3 in Appendix D. The first-stage (F-TNPS) algorithm is PS [18] as described in Algorithm 2. Accordingly, two versions, DNPS1 and DNPS2 of ordinary NPS algorithms (Algorithm 1, directly solving the original problem) corresponding to TNPS1 and TNPS2 were implemented, called. ILOG CPLEX 12.5 [35] was used as a benchmark.

All algorithms (TNPS1, TNPS2, DNPS1, and DNPS2) were implemented in C++ in the Microsoft Visual Studio 2011 environment. All test runs were carried out on a 2.67 GHz Core CPU with 4 GB RAM under Windows 7 Operating System. It seemed that no degenerate case was observed for the tested instances. In case of degeneracy, a bound-shifting technique similar to that by [36] could be applied.

5.1 Test instances

For test problems, we generated a total of 30 sites. Each site had its own generation facilities and heat and power demands. The generation facilities in each site were aggregated to 10 to 20 plants by type of plant and managed by the regional energy company. The heat and power demand and plant models were based on the history data of Finnish energy companies, similar to [29]. The CHP models were a slightly perturbed versions of rea-life plant models. Hourly power demand varied from 80 to 1100 MW and hourly heat demand from 100 to 1350 MW. The ratio of heat and power demand ranged from 0.25 to 3.5 on hourly basis and from 0.99 to 1.1 on yearly average. Energy companies in different sites operated independently. To form an interconnected system, it was assumed that two sites i and j have direct transmission line connection if $1 \leq |i-j| \leq 3$ as shown in Figure 1(b). Power transmission cost could be treated as the fee that regional generation companies pay the owner of transmission lines according to transferred quantities and congestion status of transmission lines. Generation facilities included separate plants for providing heat and power and CHP plants. 12 test problems were formed by choosing different number of sites $|F|$=3, 4, 5, 6, 7, 8, 9, 10, 15, 20, 25, and 30. For each test problem, we derived 4 variants with different structures for transmission cost and arc capacity to evaluate the impact of the symmetry for transmission cost and arc capacity on the performance of the algorithm. Consequently, a total of 48 test instances were generated. For arc ij, the transmission cost is symmetric if $c_{i,j} = c_{j,i}$ and arc capacity is symmetric if $g_{i,j} = g_{j,i}$. Let S and R denote symmetry and randomness, respectively. Pair 'SR' indicates that the transmission cost is symmetric while the arc capacity is not. For example, 3SR –site denotes a 3-site problem with "SR" structure for the transmission cost and arc capacity. Transmission costs and capacities of arcs were generated according to uniform distributions $_R$[a,b]. The range of transmission costs was [5, 30] €/MW, and the range of arc capacities was [100, 300] MW. Table 1 shows the dimensions of the 12 test problems.

5.2 Computational results

A sequence of 8760 hourly models were solved by means of TNPS1, TNPS2, DNPS1, DNPS2 and CPLEX. This is a yearly planning problem without dynamic constraints. Average results were calculated according to the 12 test instances with a specific transmission cost and arc capacity structure.

For evaluating the impact of the symmetry of transmission cost and capacity, we solved a total of 48 test

instances with 4 structures (RR, RS, SR, and SS) for the transmission cost and arc capacity. According to results, it seems that the RR structure is, on the average, the most difficult one based on the solution time. Introducing the symmetry for the transmission cost or /and arc capacity can reduce the difficulty of the problem for all algorithms. On the average, the solution time can be reduced by 3-13% for CPLEX, 3-9% for TNPS2 and 5-9% for DNPS2. However, since CPU time per iteration for NPS (TNPS1, TNPS2, DNPS1 and DNPS2) and CPLEX assume non-linear patterns (as illustrated in Figure 6), there is no definite influence pattern. In the following, due to space limits, we only report the results with the RR structure.

Table 1 Dimensions of 12 test problems

Model	Sites	Plants	Constraints	Variables	Flow variables
	$\|F\|$	$\|U\|$	m	n	n_f
3-site	3	39	45	301	6
4-site	4	57	65	444	12
5-site	5	73	83	549	18
6-site	6	88	100	659	24
7-site	7	100	114	776	30
8-site	8	114	130	875	36
9-site	9	131	149	1003	42
10-site	10	145	165	1133	48
15-site	15	216	246	1696	78
20-site	20	298	338	2340	108
25-site	25	382	432	2997	138
30-site	30	452	512	3621	168

Table 2 gives the solution time (CPU time) for all the algorithms and average number of iterations per hourly model. Figure 6 shows the patterns for the CPU time per iteration for F-TNPS (PS), TNPS and CPLEX based on the RR structure. The pattern for the CPU time per iteration for DNPS is similar to that for TNPS but it is not shown in the figure.

The solutions of the first-stage problem indicate that there is no coordination between regional systems at different sites. The numerical results show the coordination (the solution of the problem under study) can reduce cost by 5 % on the average even though a high transmission cost is imposed. This justifies the economic benefit of interconnection [12]. In the following, we focus on the solution efficiency of the algorithm.

Table 2 Solution (CPU) time and iterations per hourly model

Model	CPU						Iterations per hourly model			
	F-TNPS	TNPS		DNPS		CPLEX	F-TNPS	TNPS	DNPS	CPLEX
		TNPS1	TNPS2	DNPS1	DNPS2					
3RR-site	0.647	1.42	1.45	2.55	2.00	371.8	38.2	51.2	48.8	80.5
4RR-site	0.865	2.45	2.30	4.60	3.59	412.4	50.3	69.3	66.1	124.5
5RR-site	1.02	3.26	2.66	5.93	4.88	550.9	57.4	79.7	75.9	162.9
6RR-site	1.29	5.64	4.71	9.90	8.02	606.3	72.7	108.2	102.2	191.5
7RR-site	1.52	6.20	5.82	13.21	10.84	639.4	85.0	121.6	115.7	230.5
8RR-site	1.70	8.35	6.79	20.37	15.16	692.8	94.1	135.8	129.4	252.5
9RR-site	1.93	8.68	7.31	21.03	16.09	743.5	102.8	141.2	134.4	282.6
10RR-site	2.14	10.63	8.31	26.72	21.00	997.1	112.9	152.8	145.9	317.6
15RR-site	3.40	26.63	21.40	72.86	61.37	786.0	172.1	234.9	222.3	478.0
20RR-site	4.64	49.73	40.66	146.8	123.5	1148.4	216.7	287.3	272.4	633.3
25RR-site	6.43	95.14	78.86	302.2	259.7	1298.4	282.8	376.6	355.7	800.8
30RR-site	8.20	157.8	134.5	536.4	489.3	1606.2	343.7	451.6	426.9	964.5
Avg	2.82	34.05	28.48	105.5	92.13	861.9	135.7	184.2	174.6	376.6

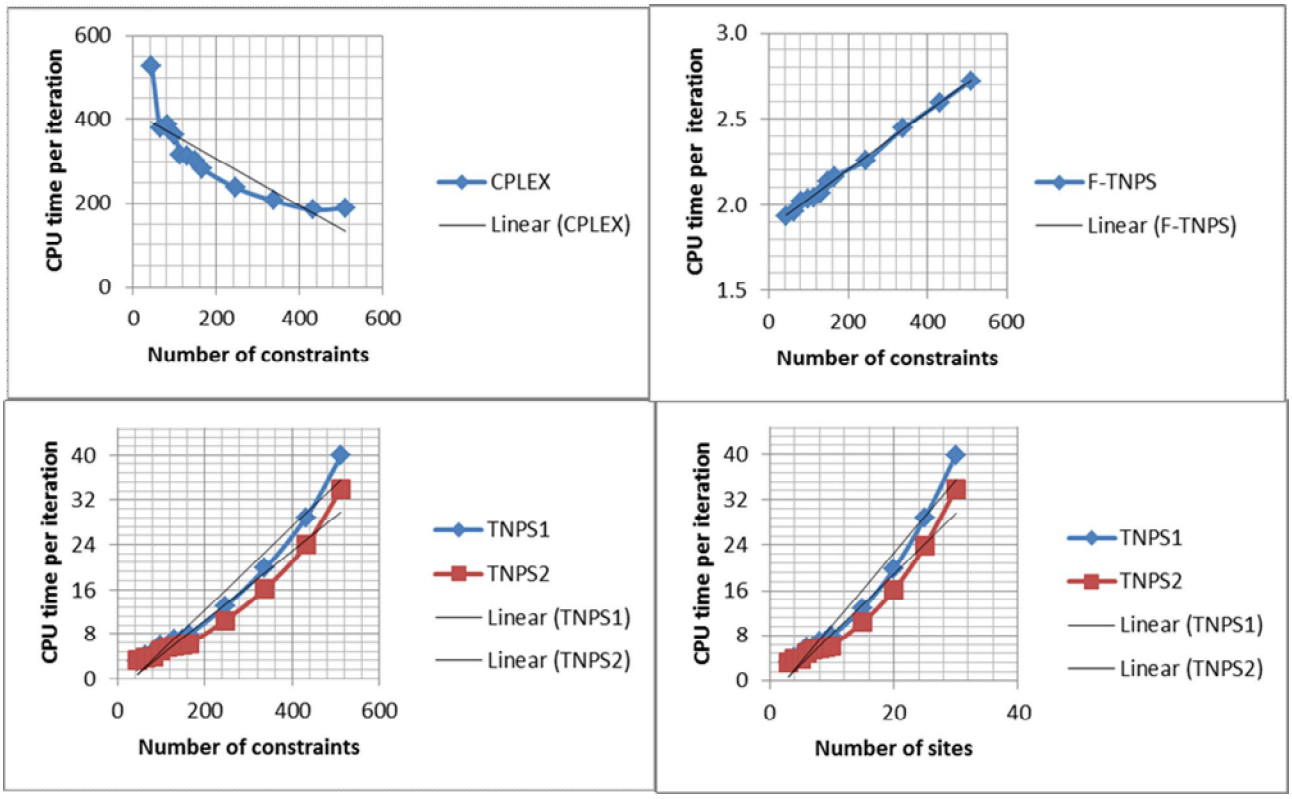

Figure 6 CPU time per iteration (μs) as a function of number of constraints (m) or number of sites ($|F|$)

From the CPU time shown in columns F-TNPS, TNPS1 and TNPS2 of Table 2, it can be seen that the first-stage problem is much easier to solve than the original problem though the size difference for these two problems is not big (m is the same and difference between n is n_f). The share of solution time for the first-stage problem consistently decreases as the number of sites increases, from nearly 50% for 3-site test problems to about 5% for 30-site problems. The same observation can be found for the pattern for CPU time per iteration in Figure 6. CPU time per iteration for F-TNPS is small and assumes a linear pattern with respect to the number of constraints (m), while CPU time per iteration for TNPS is large and increases much faster as m increases. It is worth mentioning that it is the coupling between production and transmission that contributes to the complexity of the original problem. Therefore, the complexity of the problem cannot be judged purely by $m \times n$. This can be explained from two perspectives. Firstly, in Figure 6, the pattern of CPU time per iteration against the number of sites is similar to that against m. Secondly, from Table 2, it can be seen that the solution time for the first-stage 30-site problem is close to that for 8-site original problem but the size for the former is much larger than for the latter.

According to Table 2, TNPS is on the average 3 times faster (TNPS1 against DNPS1 and TNPS2 against DNPS2) than DNPS though the number of iterations for TNPS is a little larger than that for DNPS. There are two reasons for this. Firstly, the solution obtained from solving the first-stage easy problem is not far away from the true optimum for the original problem. On the average, the relatively gap is 5%. Secondly, on the average, about 30% of iterations were spent for solving the harder second-stage (original) problem with the power network. When compared to CPLEX, TNPS is 10 (30-site problem) to 260 (3-site problem) times faster for the RR structure. On the average, TNPS1 is 25 times faster and TNPS2 is 30 times faster. For test instances with other structures for transmission cost and arc capacity, the average ratio remains more or less the same but the range changes. The largest ratio can be 360 for the 3-site instance and the smallest ratio is 7 for the 30-site instance. It seems that the CPLEX gains advantage as the problem size increases. This can be explained by the CPU time per iteration for CPLEX in Figure 6. The CPU time per iteration for CPLEX has tendency to decrease as m increases.

Finally, we evaluate the contributions of the incremental basis updates to the solution efficiency. According to Table 2, on the average TNPS improves the solution efficiency about 15% over DNPS. This improvement is not as big as expected. On one hand, incremental updates need recording the detailed information related to the pivot as mentioned in Section D.3 of Appendix D and thus incur some

bookkeeping overhead. For example, TNPS2 performs even worse than TNPS1 for the 3-site problem. On the other hand, in some iteration, the tree associated with the sites affected by the pivot contains many nodes. In this case, the benefit of the incremental updates is marginal.

6. Conclusion

Current design, planning and policy-making methodologies place too much emphasis on the role of electric power while the potential of equally important heat is ignored to a large extent. Heat accounts for 47% of final global energy demand [5]. To address power grid balance issues caused by large penetration of intermittent RES, such as solar and wind power, combined heat and power (CHP) systems (as compared with power-only systems) provide additional flexibility to influence electric power by adjusting heat production level [15] in CHP plants, by using electricity to satisfy heat demand and by using cheap heat storage [17] (as compared with electric storage) to accommodate more RES. Also an increasing interconnection of regional energy systems provides opportunities to coordinate energy scheduling among regions.

This paper has formulated the hourly transmission-constrained multi-site CHP system optimization problem as a linear programming (LP) model with a special structure and developed an efficient two-stage network Power Simplex (NPS) algorithm by exploiting the structure of the model. The numerical experiments with realistic data justify the efficiency of the algorithm. NPS is 7 to 360 (average 30) times faster than the CPLEX code. This will lay foundation for efficiently addressing more advanced CHP systems incorporating different types of storages and unit commitment to achieve high utilization of RES and for addressing investment planning for large CHP systems considering the intermittent RES, similar to large power-only systems [37].

Acknowledgement

The research was funded by the STORE (STochastic Optimization of Renewable Energy in large polygeneration systems) project (No. 298317) from Academy of Finland and the STEEM (Sustainable Transitions of European Energy Markets) project (No. 91002171) from Aalto University, Finland. We would like to thank three anonymous reviewers for their valuable suggestions to improve previous versions of the manuscripts.

References

[1] IEA (International Energy Agency). World Energy Outlook, 2014.

[2] Riipinen M. District heating and cooling in Helsinki. *International Energy Agency CHP/DHC Collaborative & Clean Energy WorkShop*, 2013.

[3] IEA (International Energy Agency). *Cogeneration and district energy—sustainable energy technologies for today and tomorrow*, 2009.

[4] Cogeneration Directive. Directive 2004/8/EC of the European Parliament and of the Council. A directive strategy to promote high efficiency cogeneration. *Official Journal of the European Union* 2004; L52: pp. 50–60.

http://www.iea.org/publications/freepublications/publication/CoGeneration_RenewablesSolutionsforaLowCarbonEnergyFuture.pdf; 2011.

[5] IEA (International Energy Agency). *Cogeneration and renewables —Solutions for a lower carbon Future*, 2011.

[6] Jaradi M and Riffat S. Trigeneration systems: Energy policies, prime movers, cooling techniques, configurations and operation strategies. *Renewable and Sustainable Energy Reviews* 2014; 32: 396-415.

[7] COGEN Europe. Cogeneration 2050—the role of cogeneration in a European decarbonized energy system.

[8] Pansini AJ. *Power transmission and distribution*. 2nd edition. Lilburn, GA: Fairmont Press; New York: Distributed by Marcel Dekker, cop. 2005.

[9] Ouyang Z and Shahidehpour M. Heuristic multi-area unit commitment with economic dispatch. IEE Proceedings-C 1991; 138(3):242-252.

[10] Streiffert D. Multi-area economic dispatch with tie lines constraints. IEEE Transactions on Power Systems 1995; 10(4):1946-1951.

[11] Li Z, Shahidehpour M, Wu W, Zeng B, Zhang B and Zheng W. Decentralized multiarea robust generation unit and tie-line scheduling under wind power uncertainty. *IEEE Transactions on Sustainable Energy* 2015; 6(4): 1377-88.

[12] Al-Shaalan AM. Technical and economical merits of power systems interconnection. Journal of Power and Energy Engineering 2013; 1-7.

[13] Siddi M. The EU's Energy Union—towards an integrated European energy market? FIIA briefing paper 172, 2015.

[14] Blarke MB and Lund H**.** Large-scale heat pumps in sustainable energy systems: System and project perspectives. *Thermal Science* 2007; 11(3):143-52.

[15] Rong A and Lahdelma R. Role of polygeneration in sustainable energy system development—Challenges and opportunities from optimization viewpoints. *Renewable and Sustainable Energy Reviews* 2016; 53:363-372.

[16] Meibom P., Kiviluoma J., Barth R., Brand H., Weber C., and Larsen HV. Value of electric boiler and heat pumps for wind power integration. Wind Energy 2007; 10:321-37.

[17] Connolly D. Heat roadmap Europe – A low- carbon heat and cooling strategy for Europe. *Summer School for District Heating and Cooling*, Helsinki, August, 2014, Finland.

[18] Lahdelma R and Hakonen H. An efficient linear programming algorithm for combined heat and power production. *European Journal of Operational Research* 2003; 148:141-51.

[19] Abdollahi E, Wang H, and Lahdelma R. An optimization method for multi-area combined heat and power production with power transmission network. *Applied Energy* 2016; 168:248-256.

[20] Dantzig G. *Linear programming and extensions*. Princeton University Press, Princeton, NJ. 1963.

[21] Rong A, Luh P, and Lahdelma R. Dynamic programming based algorithm for the unit commitment of the transmission-constrained multi-site combined heat and power system. *2016 International Conference on Power Transmission*, Paris, France, August 22-23, 2016.

[22] Tseng CL, Guan X, Svoboda AJ. Multi-area unit commitment for large scale power systems. *IEE Proceedings for Generation, Transmission and Distribution* 1998; 145(4):415-421.

[23] Ahuja RK. Magnanti TL and Olin JB. *Network flows—theory, algorithms and applications*. Prentice Hall, Upper Saddle River, New Jersey, 1993.

[24] Bertsekas, D.P. 1998. *Network optimization: continuous and discrete models*. Athena Scientific, Belmont, Massachusetts.

[25] Rong A, Hakonen H, Lahdelma R. A variant of the dynamic programming algorithm for unit commitment of combined heat and power systems. *European Journal of Operational Research* 2008; 190:741-755.

[26] Rong A, Lahdelma R, and Grunow M. An improved unit decommitment algorithms for combined heat and power system, *European Journal of Operational Research* 2009; 195:552-562.

[27] Rong A, Lahdelma R, Luh P. Lagrangian relaxation based algorithm for trigeneration planning with storages. *European Journal of Operational Research* 2008; 188:240-257.

[28] Rong A, Figueira JR, Lahdelma R. An efficient algorithm for bi-objective combined heat and power production planning under the emission trading scheme**.** *Energy Conversion and Management* 2014; 88:525-534.

[29] Rong A, Hakonen H, and Lahdelma R. An efficient linear model and optimization algorithm for multi-site combined heat and power production, *European Journal of Operational Research* 2006; 168(2), 612-32.

[30] Rong A, Lahdelma R. Efficient algorithms for combined heat and power production planning under the deregulated electricity market, *European Journal of Operational Research* 2007;176 1219-45.

[31] Rong A, Figueira JR, Lahdelma R. A two phase approach for the bi-objective nonconvex combined heat and power production planning problem**.** *European Journal of Operational Research* 2015*;* 245, 296-308.

[32] Rong A, Lahdelma R. An efficient envelope-based Branch and Bound algorithm for nonconvex combined heat and power production planning. *European Journal of Operational Research* 2007; 183, 412-31.

[33] Makkonen S, Lahdelma R. Non-convex power plant modeling in energy optimization. *European Journal of Operational Research* 2006; 171, 1113-26.

[34] Bondy JA. 1976. *Graph theory with applications*.

[35] IBM ILOG CPLEX Optimization Studio 12.5. http://ibm-ilog-cplex-optimization-studio.software.informer.com/12.5/

[36] Gill PE, Murray W, Saunders MA, Wright MH. A practical anti-cycling procedure for linearly constrained optimization. Mathematical Programming 1989; 45, 437-74.

[37] Munoz FD, Hobbs BF and Watson JP. New bounding and decomposition approaches for MILP investment problems: Multi-area transmission and generation planning under policy constraints. *European Journal of Operational Research* 2016; 248, 888-898.